Research Square

Preprints are preliminary reports that have not undergone peer review.
They should not be considered conclusive, used to inform clinical practice,
or referenced by the media as validated information.

# Experimental and Modelling Studies of Water Sorption Properties of Cellulosic Derivative Fibers.

**MATHILDE SIMON**
IMP: Ingenierie des Materiaux Polymeres
**RENE FULCHIRON**
IMP: Ingenierie des Materiaux Polymeres
**FABRICE GOUANVE** ( fabrice.gouanve@univ-lyon1.fr )
Ingenierie des Materiaux Polymeres https://orcid.org/0000-0001-9097-8106

**Research Article**

**Keywords:** water vapor sorption, hysteresis, cellulosic fiber, Park model, PEK model

**Posted Date:** June 21st, 2021

**DOI:** https://doi.org/10.21203/rs.3.rs-586610/v1

**License:** This work is licensed under a Creative Commons Attribution 4.0 International License.
Read Full License

# Experimental and modelling studies of water sorption properties of cellulosic derivative fibers.

M. Simon, R. Fulchiron, F. Gouanvé*

Université de Lyon, CNRS, UMR 5223, Ingénierie des Matériaux Polymères, UCBL, F-69622 Villeurbanne, France

## Abstract

The objective of this study was to understand the chemical modification impact on interactions between water and cellulosic fiber. In that respect, cotton (C), flax (F), viscose (V) and cellulose acetate (CA) were analyzed by using a dynamic vapor sorption analysis. The sorption and desorption isotherms and kinetic curves were modelled using the Park model and the "Parallel Exponential Kinetics" (PEK) model-which allowed an accurate fitting on the whole range of water activity. The obtained sorption properties were correlated to the accessibility and the amount of sorption sites and also to the crystallinity level of the fibers. It was found that V exhibited the highest water sorption capacity due to a higher hydroxyl groups accessibility and a high amorphous fraction, followed up by F, C and CA. In contrast, higher kinetic sorption rate was obtained for CA due to a decrease of the hydroxyl groups within the fibers. Regardless the fiber, the determination of characteristic times showed that the kinetic rate was higher for sorption than desorption.

**Keywords: water vapor sorption, hysteresis, cellulosic fiber, Park model, PEK model**

## Introduction

Cellulosic fibers have been used as structural materials since prehistoric times. More recently, interest in the use of materials derived from natural resources has increased dramatically. Environmental concerns such as global warming, energy consumption, and the desire to obtain products from renewable sources have led to a resurgence of interest in plant-derived products. Plant fibers are very attractive and are used for a wide variety of industrial applications such as textile for fabric making, automobile and building industries as reinforcement in composites materials (Ramamoorthy et al. 2015; Sanjay et al. 2019; Awais et al. 2021). They are cost-effective, renewable, available in high quantity, biodegradable, have low fossil-fuel energy requirements and can offer good mechanical properties. Natural fibers are hygroscopic materials because of high content of water sorption sites (hydroxyl groups) and deformation ability of cell wall during water exposure. Thus, physical properties such as density, shape, stiffness, crystal structure of the fibers and therefore mechanical properties (tensile modulus and breaking stress) are impacted (Célino et al. 2014). In textile industry, the hygroscopic nature allows many applications such as: absorb perspiration, transport moisture and adjust the relative humidity in the clothing microcosm.

Natural cellulosic fibers are obtained from various parts of the plants and generally classified based on the part of the plant from which they are extracted, such as seed, leaf and fruit. They are composed of various substances such as cellulose, lignin, hemicellulose and pectin. Cellulose, which is the primary reinforcing element of the cell wall, is made of linear chains of glucose residues aggregated into microfibrillar units (Awais et al. 2021). These units

possess a high crystalline content (inaccessible to water molecules) but also a paracrystalline component to which water molecules can gain access. Lignin is present in plant fibers in varying amounts; it is an amorphous crosslinked polymer composed of phenolic units. The cell wall also contains a hemicellulose and pectin component, which are predominantly amorphous polysaccharide (Hill et al. 2009). Cotton and flax fibers are the most widely used natural fibers in various fields of application. Cotton fibers are a seed fibers which are considered as the purest form of cellulose, with around 90 % cellulose content (Dunne et al. 2016). Flax fibers are a plant fiber which are composed of cellulose (80–90%), cellulosic fibrils embedded in hemicellulose (up to 7%), pectins (up to 5%) and proteins (0–1.5%). A few phenolics (1%), waxes and fats (0.5–1.0%), are also present (Kabir et al. 2012). Natural fibers can be modified using chemical treatment like alkalization (Carrillo-Varela et al. 2018), mercerization, acylation, acetylation, peroxide treatment (K. Kaushik et al. 2013), salinization and benzoylation. Those treatments affect the contents of cellulose, hemicellulose, and lignin within the fibers yielding them more amorphous. Among those, cellulose based regenerated fibers like cellulose acetate fibers and viscose fibers have attracted attention due to their more ductile behavior which allow new specific applications (Manian et al. 2018). Cellulose acetate fibers are a modified polysaccharide synthesized by the reaction of acetic anhydride with cotton linters or wood pulp (Kostag et al. 2019). In that respect, the hydroxyl groups are partially substituted by acetyl function which reduces the number of primary sorption sites (which are generally assumed to be the OH groups) (Xie et al. 2010; Popescu et al. 2014). Viscose fibers are manufactured from cotton linters or wood pulp. First cellulose is mercerized with a sodium hydroxide treatment, followed by xanthation substitution. Cellulose is then regenerated with a sulfuric acid treatment which converts cellulose into a more amorphous structure (Klemm et al. 2005) leading to higher moisture content (Okubayashi et al. 2005a).

The determination of the water uptake at equilibrium of natural fibers by the gravimetric method at a given water activity invariably uses saturated salt solutions as a means of evaluating the water sorption properties of fibers (Hill 2006). In recent years, dynamic vapor sorption (DVS) technique has been used to investigate the sorption and desorption of natural or regenerated cellulosic materials from a thermodynamic point of view (Jonquières and Fane 1998). This technique leads to reproducible data and can provide accurate isotherms for water activities up to 0.95. Recent studies have not allowed a perfect understanding of water sorption behavior of cellulosic fibers. Two main factors can explain this issue: the complex internal geometry of the cell wall and the continuous nano-structural changes associated with the dynamic behavior of the cell wall macromolecular components. In order to understand sorption mode and possible interactions between water molecules and cellulosic fibers, sorption models have been established (Leung 1983). Those models described water sorption isotherms of cellulosic materials, nevertheless they are limited in the fitting of the experimental data for the whole range of water activities and for all types of cellulosic materials. This limitation on the fitting has been attributed by Labuza (Labuza 1980) to different mechanisms of water association with cellulosic fibers in different water activity regions. Depending on the nature of the fiber, some models are more or less relevant. The Ferro-Fontan model allows to predict sorption isotherm in 90% of cellulosic products (Chirife et al. 1980). Peleg suggests a four parameters model, which can be used for both sigmoidal and non-sigmoidal isotherms (Peleg 1993). The Smith model is convenient for sorption isotherms of biological materials, such as starch (Smith and Smith 1947). Chirife and Iglesias found that Halsey and Oswin models are also versatile for the description of polysaccharide systems (Iglesias and Chirife 1976). The well-known GAB model based on multilayers and condensed systems is considered to be one of the most versatile model for water sorption in cellulosic materials (GAB model, Guggenheim-Anderson-de Boer) but failed to fit

values obtained at high water activity (higher than 0.9) (Guggenheim 1966). The Park model is more convenient to fit the water sorption isotherms in the whole range of water activity. This model corresponds to a multi-sorption mode, which can be dividing in three steps: (1) Langmuir sorption, (2) Henry's law, and (3) water clustering (Park 1986).

The ability of the DVS technique to collect experimental data in real time, allows the sorption analysis of the fibers in a kinetic point of view. Different authors have shown that the water sorption kinetics in cellulosic fibers was not Fickian (Van Der Wel and Adan 1999; Krabbenhoft and Damkilde 2004). Fickian models are based on two assumptions. First, transfer of water molecules is governed by a Fickian type gradient law. Secondly, for natural fibers, there exists an equilibrium state such that the water content is at all times a unique function of the corresponding water activity as given by the sorption isotherm. The first assumption that the flux of some quantity can be taken as being proportional to the gradient of this quantity by some scalar diffusion coefficient is probably reasonable when dealing with a relatively slow transfer under isothermal conditions. However, the second assumption that there is instantaneous equilibrium between the bound water and the water vapor at all times is harder to justify. Kohler et al.(Kohler et al. 2003, 2006) have reported that water exchange of cellulosic fibers, can be modelled by two parallel independent first order processes, which was defined by the "Parallel Exponential Kinetics" (PEK) model. This model assumes two different mechanisms for the exchange of water vapor relating to different sorption sites. Several assumptions have been established to describe the two-basis behavior of PEK model. Kohler *et al.* (Kohler et al. 2003, 2006) suggested that the fast kinetic process is associated with the formation of the monolayer or "bound" water and the slow kinetic process is assigned to the multilayer or "free" water. Okubayashi *et al.* (Okubayashi et al. 2004, 2005a, b) connected these two processes to water sorption sites accessibility. Thus, the fast-kinetic process is related to the sorption of "amorphous" regions and accessible internal surfaces, whereas the slow kinetic process is attributed to "inner" surfaces and "crystallites" sorption. Hill (Hill et al. 2010a, b, c) and Xie (Xie et al. 2010, 2011c, b; Hill and Xie 2011) connected the fast sorption process to readily accessible sorption sites in the cell wall internal surface, whilst the slow process is linked to the production of new sites as the cell wall expands or the loss of these sites as the cell wall contracts. Guo *et al.* (Guo et al. 2017) confirmed this hypothesis. Besides an excellent fit to the experimental data, it provides a set of easily interpretable, physically meaningful parameters.

In this present work, a comparative study of water sorption and desorption of two natural cellulosic fibers, cotton and flax, and two regenerated cellulosic fibers, cellulose acetate and viscose is presented and discussed. The obtained isotherms were modelled using the Park model in order to have information about the sorption mode and the interactions between water molecules and cellulosic fibers at different water activity. The sorption and desorption kinetic curves were analyzed using the PEK model. A discussion of the physical interpretation from the fast and slow sorption processes of the PEK model is also presented. The obtained sorption properties results were correlated to the accessibility and the amount of sorption sites and also to the crystallinity level of the fibers.

# Experimental

## Materials

Four cellulosic materials, cotton (C), flax (F), viscose staple (V) and cellulose acetate (CA) supplied by *Les Tissages de Charlieu* (Charlieu, France), were used in the experiments. Degree of substitution (DS) of CA was determined using the procedure described by Rodrigues et al. (Rodrigues Filho et al. 2008). The characteristics of the fibers are given in Error! Reference source not found., and the chemical structure of cellulose and CA are in **Fig. 1**.

**Table 1** Mass percentage of the various constituents of various cellulosic and derivative fibers

| Material | Mass composition (%) | | | | Function | DS | Ref |
|---|---|---|---|---|---|---|---|
| | Cellulose | Hemicellulose | Pectin | Lignin | | | |
| **C** | 82-99 | 3-6 | 0-5.7 | - | - | | (Bledzki and Gassan 1999; Olesen and Placket 1999; Lilholt and Lawther 2000; Mohanty et al. 2000) |
| **F** | 64-85 | 10-20.6 | 2.3-12 | 0-5 | - | | |
| **V** | 100 | - | - | - | - | - | (Klemm et al. 2005) |
| **CA** | 100 | - | - | - | Acetate | 2,1[a] | (Rodrigues Filho et al. 2008) |

a: obtained by titration according to previously published procedures (Rodrigues Filho et al. 2008)

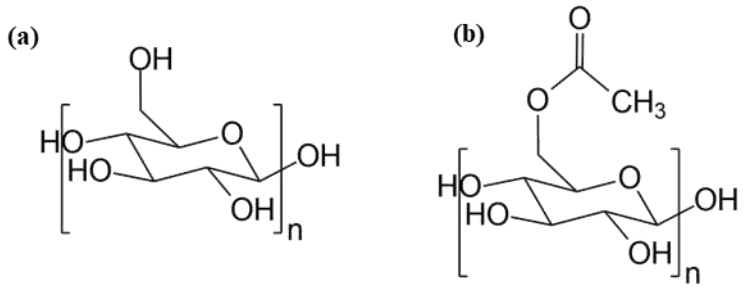


**Fig. 1** Chemical structure **(a)** cellulose (French 2017), **(b)** cellulose acetate in cellulosic fibers

## Optical microscopy

Microscopy images were obtained using a Leica M205A stereomicroscope with greater sample depth, Planapo1.0x objective and magnification x150.

### Infrared Spectroscopy (FTIR)

FTIR spectra were recorded on a Nicolet iS10 infrared spectrometer from Thermo Fischer Scientific in attenuated total reflectance (ATR) mode with a diamond crystal. The scanning was conducted in the wave number range of 4000-400 $cm^{-1}$ with a 64 repetition scans for each sample. The resolution was set at 4 $cm^{-1}$ during the measurement.

## Wide-angle X-ray scattering (WAXS)

WAXS analyses in reflection (Bragg-Brentano) mode were carried out at room temperature using a Cu tube ($\lambda = 1{,}54\ Å, 40\ kV, 40\ mA$) and a nickel filter in order to remove the Kβ line and a Bruker D8 Advance diffractometer

with a Bragg-Brentano configuration. The diffraction patterns were obtained in a $2\theta$ range between 5° and 50° by step of 0.02°. Fibers were deposited on corundum substrate with a thin transfer adhesive of low scattering response.

Crystallinity index ($X_c$) was determined by deconvolution method. $X_c$ which is defined as the ratio of the sum of area of cellulose crystalline peaks ($A_{cr}$) to the sum of the area of the total peaks of sample material including amorphous part ($A_{am}$) as defined by the following equation **(Eq. 1)**:

$$X_c(\%) = \frac{A_{cr}}{A_{cr} + A_{am}} \times 100 \qquad \textbf{Eq. 1}$$

### Vapor water sorption

Water sorption isotherms of the different fibers were determined at 25 °C by using the dynamic vapor sorption analyzer (DVS Advantage, London, United Kingdom). The vapor partial pressure was controlled by mixing dry and saturated nitrogen, using electronic mass flow controllers. The initial mass of the samples was between 15 to 40 mg. Each sample was pre-dried by exposure to dry nitrogen until the dry mass was obtained ($m_0$). A partial pressure of vapor ($p$) was then established within the apparatus and the mass of the sample ($m_t$) was followed as a function of time. The mass of the sample at equilibrium ($m_{eq}$) was considered to be reached when changes in mass with time ($dm/dt$) were lower than $2.10^{-4}$ %.min$^{-1}$ for at least 10 consecutive minutes. Then, the samples were exposed to the following water activity (0.05, 0.10, 0.20, 0.30, 0.40, 0.50, 0.60, 0.70, 0.80, 0.90 and 0.95), before decreasing to 0 in the reverse order. The value of the mass gain at equilibrium ($M$) defined as $(m_t - m_0)/m_0$ for each water activity ($a_w$) allowed plotting the water sorption and desorption isotherms for each sample.

## Theory

### Thermodynamic analysis

The mathematical description of the sorption isotherms can bring useful information concerning the sorption mode and the interactions involved in the sorption process (Leung 1983; Farahnaky et al. 2009). Several models have already been used to describe sigmoidal type isotherms. These models are classified into three different groups (Iglesias and Chirife 1976): (i) empirical models (like Smith, Oswin and Peleg models), (ii) semi-empirical models (like Ferro-Fontan, Henderson and Halsey models) and (iii) models based on a multi-layer approach (Modified-Brunauer, Emmett, Teller (BET) model and GAB model) (Al-Muhtaseb et al. 2004). Park has proposed a model which offers a detailed description of sorption phenomena by expressing $M$ versus $a_w$ (Park 1986). This model comprises three terms, **(Eq. 2)**:

$$M = \frac{A_L b_L a_w}{1 + b_L a_w} + k_H a_w + K_a a_w^n \qquad \textbf{Eq. 2}$$

The first term describes Langmuir sorption which leads to a plateau of concentration when water activity increases, corresponding to the saturation of the specific sites of sorption. Langmuir's terms, $A_L$, (Langmuir capacity constant) and $b_L$ (Langmuir affinity constant) have an influence in the first step of water sorption, at low water activity. The second term defines a linear evolution of the mass gain when the water activity increases (Henry's law). Henry's solubility coefficient, $k_H$, defines the slope of the isotherm in the second zone. The third term is a

power function which represents the water aggregation phenomenon. The two last parameters, $K_a$, the equilibrium constant for the clustering reaction and, $n$, the mean number of water molecules per cluster can be linked to the equilibrium state corresponding to the aggregate formation in the last zone at high water activity:

$$zH_2O \overset{Ka}{\Leftrightarrow} \frac{z}{n}(H_2O)^n.$$

with $z$, the total number of water molecules sorbed. However, it should be noted that the $n$ value represents a fitting parameter related to the mathematical calculation of the Park model and thus may be different of the real mean cluster size which was determined at different activity using Zimm and Lundberg theory.

To evaluate the accuracy of Park model to describe the experimental water sorption isotherms of the different fibers, the coefficient of determination ($R^2$) and the standard error of estimate ($SE$) were used. $SE$ is defined by the following equation **(Eq. 3)**:

$$SE = \sqrt{\frac{\sum_{i=1}^{n}(m_i - m_{pi})^2}{N}} \qquad \textbf{Eq. 3}$$

where $m_i$ is the experimental value, $m_{pi}$ is the predicted value, and $N$ is the number of experimental data. $R^2$ values close to unity and low values of $SE$ mean that the model is able to explain the variation in the experimental data. The parameters of Park equation were determined by fitting using the software Origin 9.1.

## Kinetics analysis

A change of water vapor activity around the sample (from $a_{wi}$ to $a_{w(i+1)}$) induced its water content to change with time until a new equilibrium is reached. Diffusion is a process by which water molecules are transported from one part of a system to another one as a result of random molecular motions. The molecules first dissolve in the polymer and subsequently diffuse through the polymer. It has been shown that the water vapor sorption kinetics of cellulosic fibers is not Fickian (Van Der Wel and Adan 1999; Krabbenhoft and Damkilde 2004). Kohler *et al.* (Kohler et al. 2003, 2006) have reported that water exchange of cellulosic fibers, can be modelled by two parallel independent first order processes constituting the "Parallel Exponential Kinetics" (PEK) model. This model assumes two different mechanisms for the exchange of water vapor relating to different sorption sites. Besides an excellent fit to the experimental data, it provides a set of easily interpretable.

According to their method, experimental moisture content is simulated as a function of time as described in the equation below **(Eq. 4)**:

$$M_t = M_{fast}\left(1 - e^{-t/t_{fast}}\right) + M_{slow}\left(1 - e^{-t/t_{slow}}\right) \qquad \textbf{Eq. 4}$$

Where, $M_t$ is the water content at time $t$, $M_{fast}$ $M_{slow}$ are water contents at infinite time and $t_{fast}$ $t_{slow}$ are characteristic times for the two kinetic process. Subscripts 1 et 2 indicate the two kinetic processes defined as fast and slow, corresponding to slow and fast sorption sites. The fast-kinetic process has been proposed to be related to the fast moisture sorption at the sites of "external" surfaces and "amorphous" regions, whereas the slow-kinetic process has been related to the sorption of "inner" surfaces and "crystallites" (Okubayashi et al. 2005b).

## Results and discussion

### Optical microscopy

The morphology of derivatives cellulosic fibers obtained by optical microscopy are seen in **Fig. 2**. The V, F, C fibers consist of multifilament twisted. CA fibers are oriented. Similar images have been found in the literature by Arbelaiz et al. and Mozdyniewicz et al. 2016.(Arbelaiz et al. 2005; Mozdyniewicz et al. 2016).

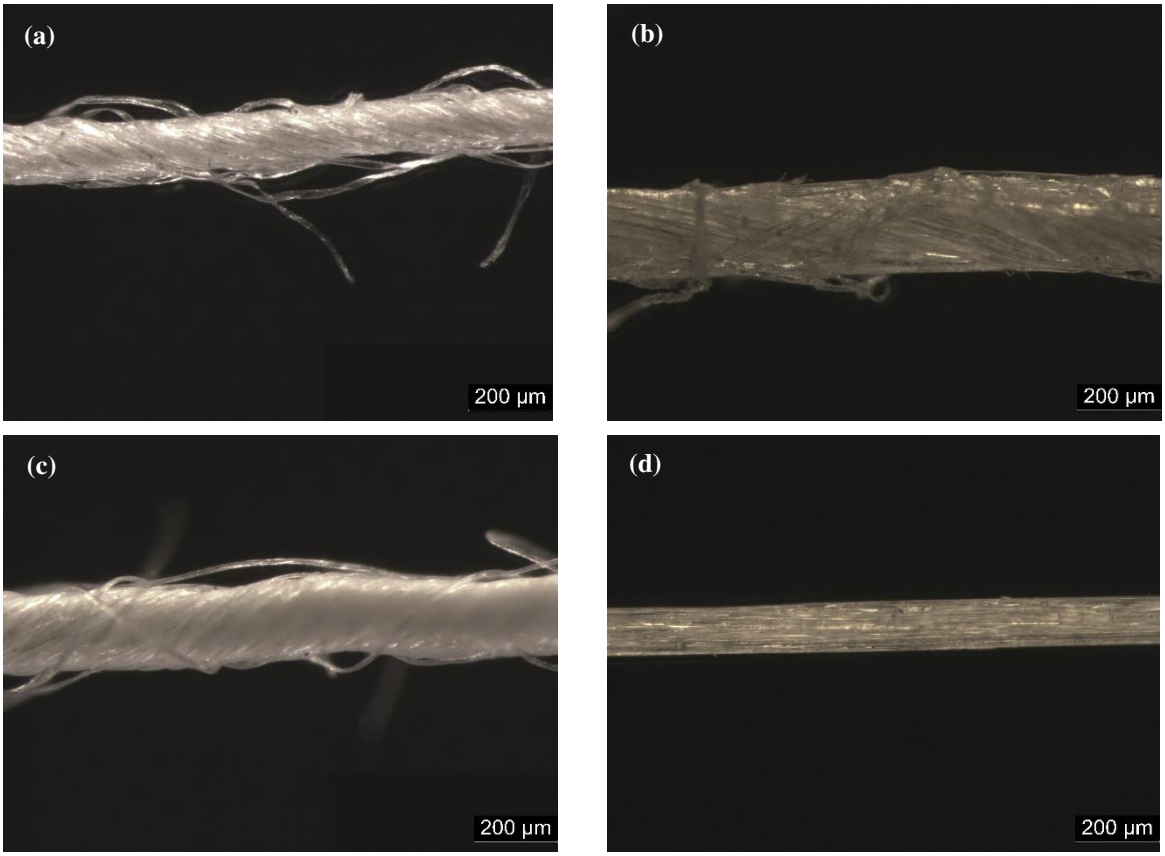


Fig. 2. Optical microscopy picture of (a) cotton, (b) flax, (c) viscose staple and (d) cellulose acetate fibers (Gx150)

### Chemical structure

The chemical composition of C, F, V and CA fibers was analyzed using FTIR-ATR. The interesting peaks are identified in **Fig. 3**. C, V and F fibers have a similar chemical footprint (Alix et al. 2009; Célino et al. 2013; Abidi et al. 2014). The broad absorption band between 3600 and 3000 $cm^{-1}$ is the characteristic of the O-H stretching vibration and hydrogen bond of the hydroxyl groups. The band at 1630 $cm^{-1}$ was assigned to bending mode of the adsorbed water. The peak at 1460 $cm^{-1}$ corresponds to the OH bending and that at 1160 $cm^{-1}$ related to the C-O antisymmetric bridge stretching (Das et al. 2014). The absorption band at 1311 $cm^{-1}$ was assigned to $CH_2$ stretching. In addition, the non-cellulosic polysaccharides were almost completely eliminated, as indicated by the absence of a peak at 1210 $cm^{-1}$.

The spectrum of CA fibers provides strong evidence of acetylation by showing the presence of three important ester bonds at 1730 $cm^{-1}$ (C =O ester), 1367 $cm^{-1}$ (C-H bond in -O-CO-$CH_3$ group) and C-O stretching band of

acetyl group at 1220 $cm^{-1}$ (Das et al. 2014). The intensity of the broad band at 3400 $cm^{-1}$ assigned to the stretching of the hydroxyl group decreased for CA compared with natural cellulose. A strong band at 1051 $cm^{-1}$ was due to the C-O-C pyranose ring skeletal vibration. Another important aspect observed in the CA spectrum was the decreasing absorption intensity of the band located at around 3400 $cm^{-1}$ assigned to the stretching of the hydroxyl group when compared with C or F.

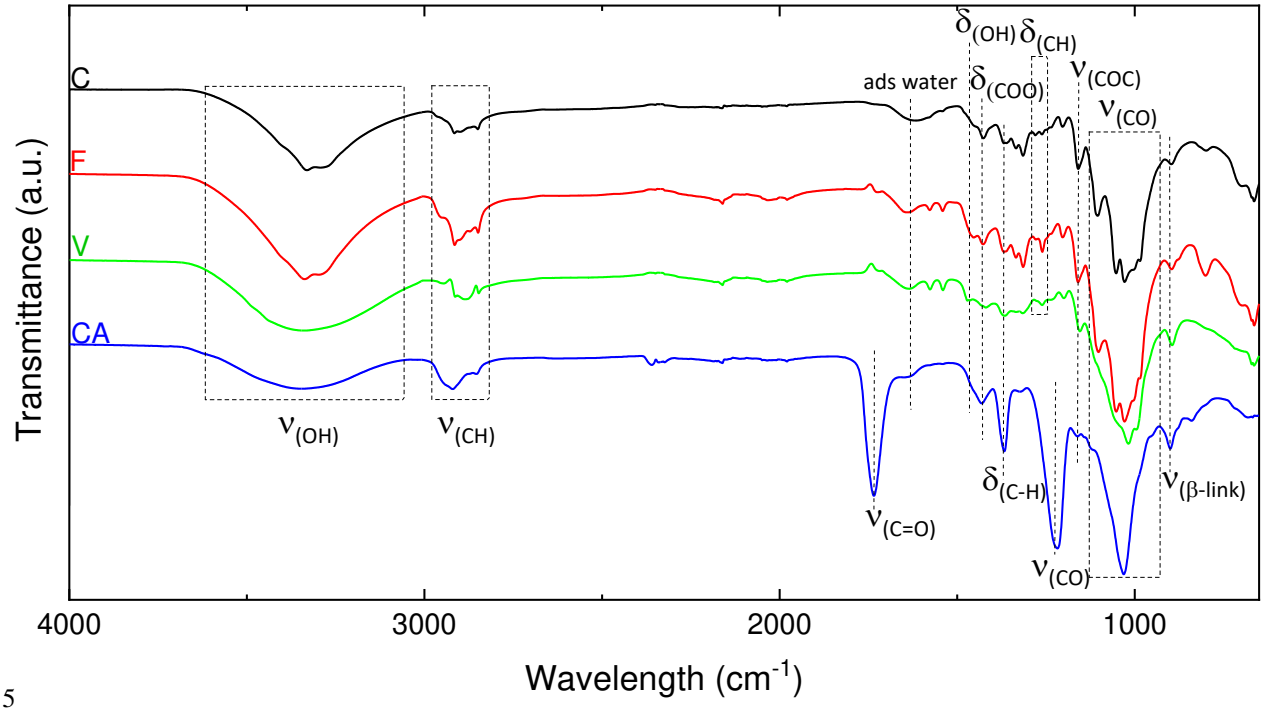


**Fig. 3** FTIR spectra of C, F, V, CA fibers

## XRD measurements

XRD analyzes were performed in reflection mode. The obtained XRD patterns are presented in **Fig. 4**. The diffraction diagrams of C and F fibers are consistent with the description of natural cellulose provide by French (French 2014). The diffraction peaks show five diffractions peaks at $2\theta$ = 14.9°, 16.7°, 21.0°, 22.7° and 34.7° and were assigned to the diffraction planes $(1\bar{1}0)$, (110), (102), (200) and (004) respectively (Park et al. 2010; Duchemin et al. 2012; French 2014; Kafle et al. 2014). These peaks belong to cellulose $I_\beta$ crystalline structure.

The diffraction diagram of V fiber show three peaks at $2\theta$ = 12.5°, 21.0° and 22.2° assigned to the $(1\bar{1}0)$, (110), (020) planes respectively (Hindeleh and Johnson 1974; Ibbett et al. 2008; Karacan and Soy 2013; French 2014; Kafle et al. 2014; Kale et al. 2020) and were related to the cellulose II crystalline structure after mercerization (Kafle et al. 2014). An additional peak is observed at $2\theta$ = 25.4° and was assigned to the anatase phase of titanium dioxide ($TiO_2$) which gives a white coloration to the V fiber (Reddy et al. 2003).

The XRD pattern of CA show a diffraction peak around 9.1◦ attributed to the crystalline peaks of CA II (Deus et al. 1991). In addition, a diffraction peak at around 19.7◦, which was commonly assigned to the less ordered or amorphous region of the cellulose chains (Freire et al. 2006).

A deconvolution procedure was applied on the XRD patterns according to the position of the different peaks defined previously, using the open software Fityk. The diffraction pattern can be decomposed into a broad amorphous halo centered at $2\theta = 19.5°$ and Gaussian functions for each crystalline peak (Ibbett et al. 2008; Terinte et al. 2011; Wu et al. 2014). The curves resulting from the deconvolution are presented in Supporting information, section **SI1** and allow quantifying the degree of crystallinity ($X_c$). Cellulosic fibers from various plants and different treatments differ considerably in their crystallinity index, as evidenced by a large number of investigative methods (Thygesen et al. 2005; Park et al. 2010; Terinte et al. 2011). Consequently, $X_c$ values were calculated for each fiber and the data are listed in **Table 2**.

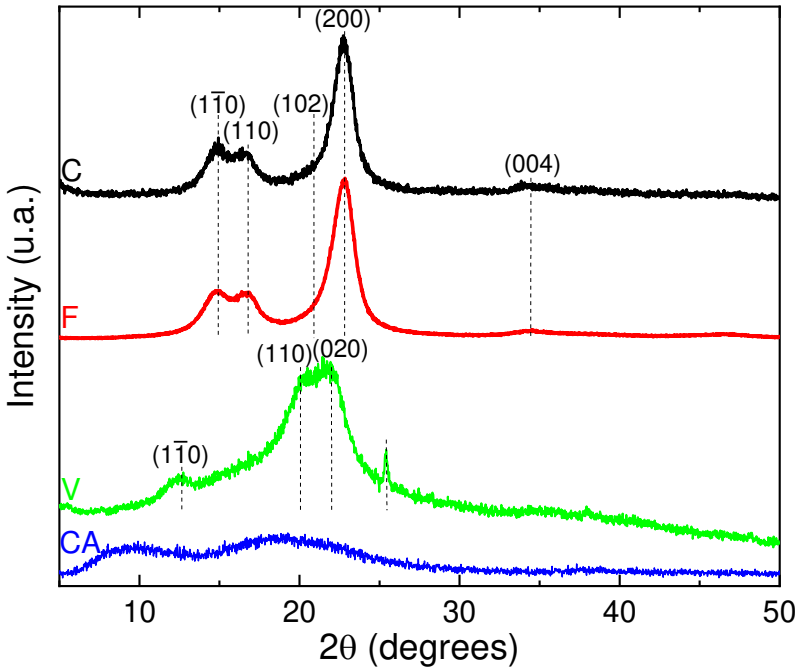


**Fig. 4** WAXS patterns of C, F, V and CA fibers

**Table 2** Crystallinity index of the fibers

| Material | $X_c$ (%) |
|---|---|
| **C** | 61 ± 3 |
| **F** | 67 ± 2 |
| **V** | 34 ± 1 |
| **CA** | < 15 |

C and F fibers had a crystallinity index up to 60 %, with 61 and 67 % respectively. The obtained values of $X_c$ were in good agreement to those obtained by Yueping et al. and Mikhalovska et al. (Yueping et al. 2010; Mikhalovska et al. 2012). The cellulosic derivatives display a low crystallinity index compared to the native cellulose ($X_c$ = 34 % and less than 15 % for V and CA, respectively). The decrease of crystallinity of CA has been explained by the fact that the substitution of the hydroxyl groups by acetyl with greater volume, break the inter- and intra-molecular hydrogen bonds of cellulose (Hu et al. 2011; Das et al. 2014) and the decrease of crystallinity of V was attributed to the mercerization treatment as explained by Kafle *et al.*(Kafle et al. 2014). Variations in the crystallinity of fibers can influence their textural characteristics, especially during interactions with water resulting in swelling.

## Water vapor sorption

### *Sorption isotherms*

The hydrophilic behavior of cellulosic materials depends on their composition and their structural properties (Célino et al. 2014). Cellulosic derivatives have hydroxyl groups on cellulose, hemicellulose and lignin which are able to establish hydrogen bond with water molecules. Moreover, a water vapor sorption occurs on non-crystalline areas and crystalline surfaces (Okubayashi et al. 2004). It has already been demonstrated that the crystallinity and the amount of hydrophilic sites could play a significant role on the water sorption behavior of fibers (Mihranyan et al. 2004).

Individual moisture sorption/desorption isotherms are shown in **Fig. 5** for the following fibers: C **[Fig. 5(a)]**, F **[Fig. 5(b)]**, V **[Fig. 5(c)]** and CA **[Fig. 5(d)]**. The sorption and desorption isotherm curves for all fibers have a sigmoid or S-shape, which corresponds to the type II in the classification of BET. This behavior is very typical of cellulosic-based materials (Hill et al. 2009; Célino et al. 2014) and can be generalized to many hydrophilic materials (Sabard et al. 2012; Ormondroyd et al. 2017). The sorption and desorption isotherms of CA fiber had a less pronounced sigmoid shape compared to the others fibers. This can be explained by a decrease of the amount of sorption sites because hydroxyl groups are substituted by acetyl groups leading to a decrease of available sorption sites (Gocho et al. 2000; Beever and Valentine 2007; Masclaux et al. 2010; Cunha et al. 2014; Himmel and Mai 2016).

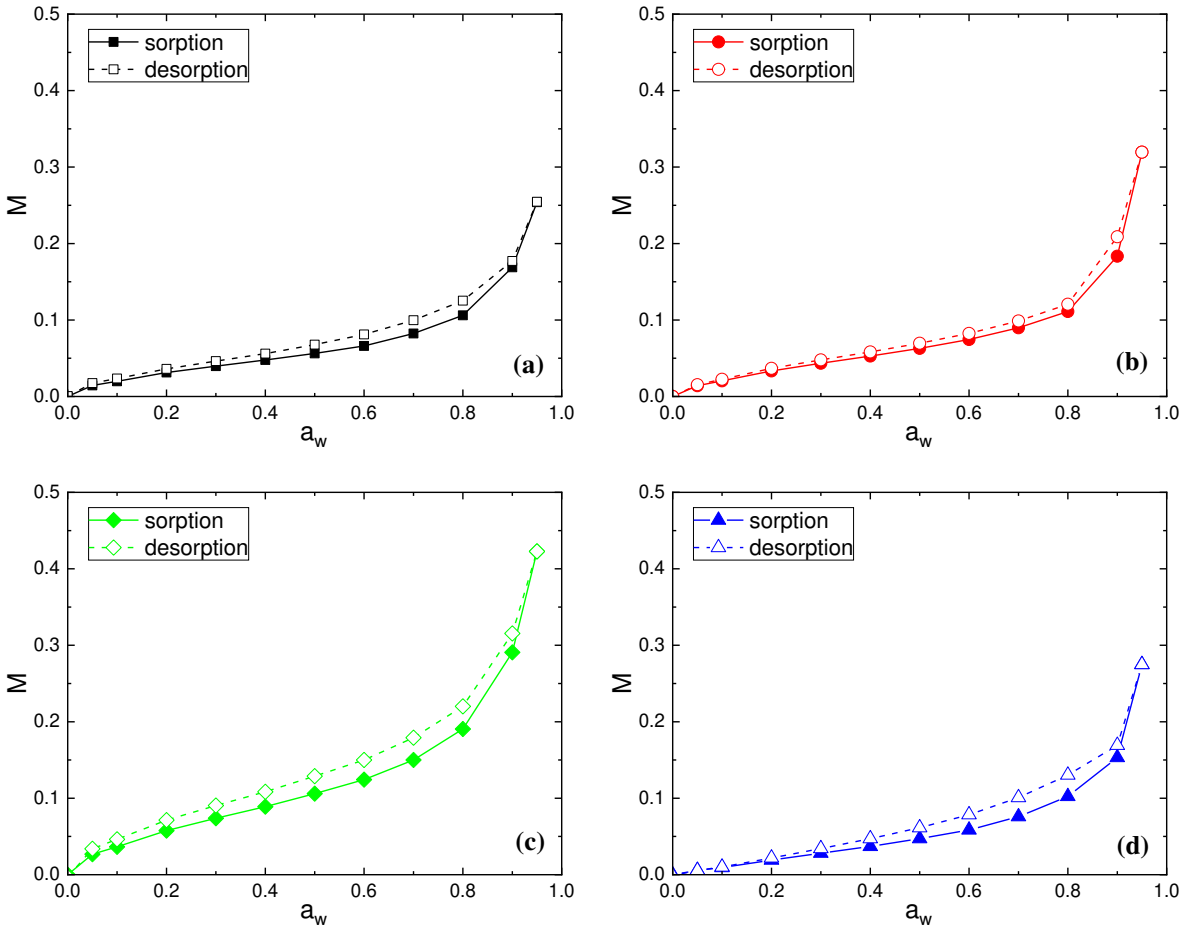


**Fig. 5** Water isotherms of **(a)** C, **(b)** F, **(c)** V and **(d)** CA fibers

The differences in sorption and desorption behavior are more clearly illustrated when the curves are overlaid in **Fig. 6(a)** (sorption) and **Fig. 6(b)** (desorption).

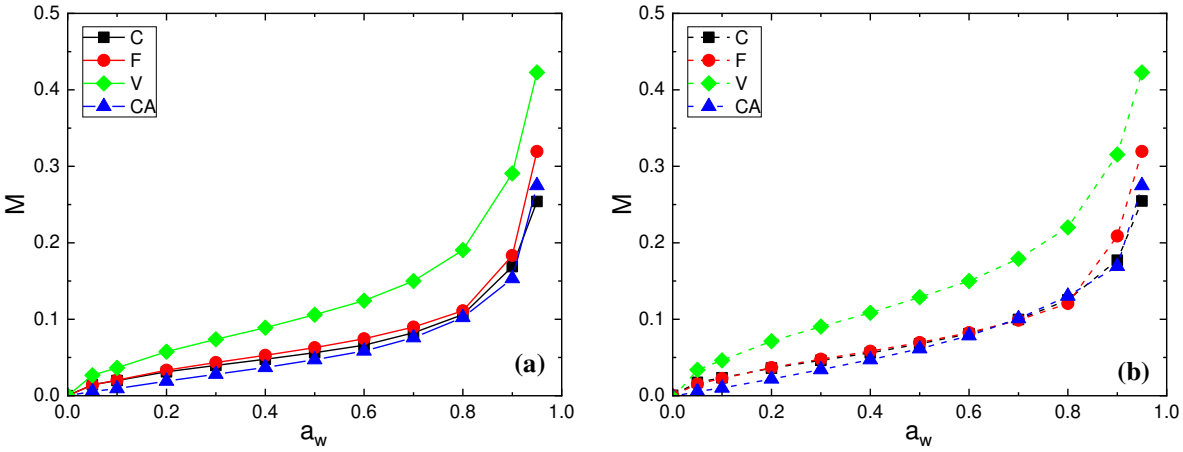


**Fig. 6** Water **(a)** sorption and **(b)** desorption of C, F, V and CA fibers

V exhibited higher water sorption and desorption capacities because of large number of free hydroxyl groups presented in regenerative cellulose and a relatively low crystallinity index ($X_c$ = 34%). Then, F and C fibers had close water sorption and desorption uptakes in the whole range of water activity. Despite a higher crystallinity index, F fiber had a slightly higher level of water uptake compared to C fiber. This result is in agreement with this obtained by Mikhalovska *et al.* (Mikhalovska et al. 2012) and was explained by the presence of lignin in F fiber which was able to participate to the water sorption process. According to Hill *et* al., the reason why more highly lignified fibers show a higher water uptake may be related to the ability of the lignin network to accommodate water within the cell wall. The hydroxyl groups content to unit mass ratio is lower than with cellulose, thus OH accessibility would be higher in lignin compared with cellulose (Hill et al. 2009). Cellulose acetate, due to the hydroxyl substitution into acetyl groups, exhibited the lowest water concentration despite its low crystallinity. Therefore, it appears that not only the crystallinity but also swelling and sorption sites amount affected water sorption capacity of cellulosic fibers.

To further understand the sorption and desorption mechanisms, Park's model was used according to **Eq. 2**. The Park's model is consistent with a multistep sorption mode, usually observed for hydrophilic polymers and can be divided into three terms. The Langmuir-type sorption relates to the sorption of the first water molecules on specific sorption sites within fibers. The Henry type law sorption describes the random dissolution of sorbed water molecules in the polymer for an intermediate water activity range. The third term corresponds to the water aggregation displayed by an exponential change in water mass gain. The values of the Park parameters for the all the fibers are summarized in **Table 3**. The examination of ***SE*** and $\boldsymbol{R}^2$, indicates that the Park's model can be used to describe the experimental sorption and desorption isotherms with a good accuracy.

**Table 3** Sorption and desorption parameters of Park determined from water sorption isotherm of the fibers

| Material | | $A_L$ | $b_L$ | $k_H$ | $K_a$ | $n$ | $SE$ | $R^2$ |
|---|---|---|---|---|---|---|---|---|
| **C** | S | 0.0100 | 60 | 0.090 | 0.290 | 13 | $1.8\times10^{-3}$ | 0.987 |
| | D | 0.0100 | 60 | 0.120 | 0.260 | 14 | $1.3\times10^{-3}$ | 0.996 |
| **F** | S | 0.0102 | 81 | 0.107 | 0.516 | 18 | $1.7\times10^{-3}$ | 0.999 |
| | D | 0.0106 | 70 | 0.126 | 0.504 | 18 | $1.1\times10^{-3}$ | 0.997 |
| **V** | S | 0.0311 | 35 | 0.152 | 0.387 | 10 | $2.3\times10^{-3}$ | 0.997 |
| | D | 0.0317 | 38 | 0.202 | 0.377 | 12 | $1.7\times10^{-3}$ | 0.999 |
| **CA** | S | 0.0000 | 0 | 0.104 | 0.456 | 19 | $4.7\times10^{-3}$ | 0.996 |
| | D | 0.0000 | 0 | 0.125 | 0.447 | 18 | $6.0\times10^{-3}$ | 0.982 |

An example of plotting of isotherm sorption curve showing the three mode contributions is reported in **Fig. 7** for the V fiber.

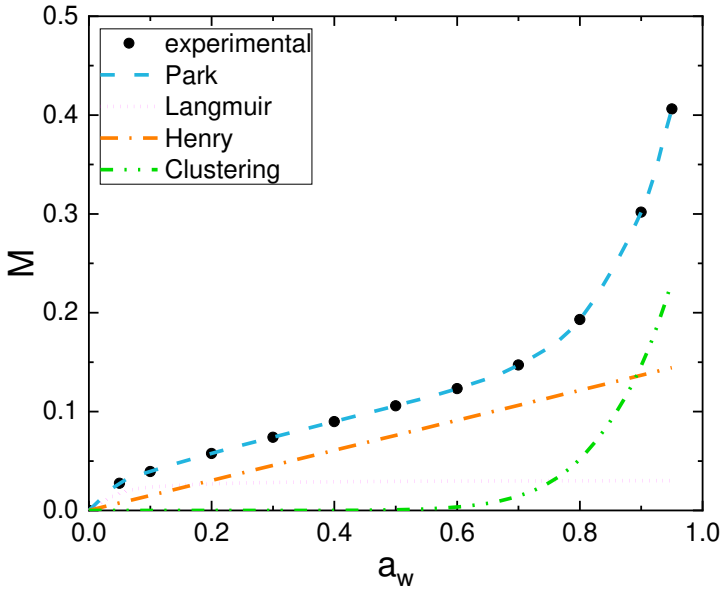


**Fig. 7** Experimental results and Park fit to experimental sorption isotherms for V staple fibers

Regarding the analysis of the Park model parameters, the chemical composition and the crystallinity index of cellulose have an influence on the three sorption modes. About the Langmuir mode, the evolutions of mass gain for all the fibers are shown in Supporting information, section **SI2a.** The parameter $A_L$ which defines the Langmuir capacity corresponds to the value at the plateau whereas the Langmuir affinity constant $b_L$ governs the water activity where the plateau is reached. $A_L$ and $b_L$ values of CA are close to zero due to a low amount of Langmuir sorption sites and the presence of acetyl groups. F and C exhibit close values of $A_L$ and $b_L$ respectively due to the same amount of hydroxyl groups in both fibers and the same water affinity for the specific groups. The activity to reach the plateau for these fibers was around 0.2. V exhibits the highest value $A_L$ because of the presence of a large accessible number of free hydroxyl groups presented in regenerative cellulose and $b_L$ value is lower compared to those obtained for F and C with a water activity to reach the plateau around 0.4.

The evolutions of the mass gain of the Henry sorption mode as a function of the water activity for all fibers are shown in Supporting information, section **S2b**. The curves show a linear increase and the slope value is the Henry's solubility coefficient $k_H$. The $k_H$ values exhibit an ascending sequence for C, CA, F and V, respectively. The $k_H$ parameter value defined as the random sorption of the water molecules in the fibers can be related to the level of amorphous phase, the presence of lignin and the amount of free volume of the fiber (Gouanvé et al. 2006).

The third term corresponding to the water aggregation phenomenon, displayed by an exponential change in water mass gain as a function of the water activity, as seen in Supporting information, section **S2c**. The $K_a$ values (equilibrium constant for the clustering mechanism) and $n$ (mean number of water molecules per cluster) can be linked to the equilibrium state corresponding to the formation of water molecules aggregate at high water activity. V fibers exhibit the highest water sorbed molecules in an aggregation state. For the other fibers, close values were obtained up to $a_w = 0.9$ and differed at $a_w = 0.95$ with a descending sequence for F, CA and C.

Park's parameters were compared for the sorption and desorption isotherms for each fiber. Regardless the fiber, differences were obtained only for the Henry sorption mode where a higher value of $k_H$ was obtained for the desorption isotherms. No significant differences were observed for the $A_L$, $b_L$, $K_a$ and $n$ meaning that Langmuir and water aggregation modes were not depended on the sorption or desorption mode.

*Sorption kinetics*

The sorption and desorption kinetic behavior of the different fibers was also studied using the "Parallel Exponential Kinetics" model (PEK-model). The interpretation of this model, is the existence of two distinct sorbent sites, with different accessibilities for water vapor, according to the different characteristic times $t_{Fast}, t_{Slow}$ and with different sorption capacity given by the equilibrium masses $M_{\infty Fast}$ and $M_{\infty Slow}$. According to Xie *et al.*(Xie et al. 2011a), the fast kinetic process has been related to the sorption at the sites of the readily accessible internal surfaces and 'amorphous' regions, while the slow kinetic process has been related to sorption onto the 'inner' surfaces and 'crystallites' (Okubayashi et al. 2004). This hypothesis has been tested and reported upon previously and it was concluded that there is little evidence supporting this idea (Bessadok et al. 2009; Xie et al. 2010; Belbekhouche et al. 2011; Hill and Xie 2011). For illustration, examples of fitting, exhibiting the contributions of slow and fast processes, is reported in **Fig. 8** for C in the activity range from 0.2 to 0.3 and 0.4 to 0.3 for sorption and desorption respectively. The model is suitable to describe the experimental sorption and desorption kinetic curves considering both contributions. The values of the parameters of the PEK model for sorption and desorption were determined at each water activity for the whole fibers. A comparison of the characteristic time coefficients extracted from the modelling in all the range of activity are shown in **Fig. 9**. For C, F and V, $t_{Fast}$.and $t_{Slow}$ for sorption and desorption showed a similar trend. The times decreased at low water activity (0.05 to 0.2), remained relatively constant in the medium range activity (0.2 to 0.6) and then increased at high water activity (0.6 to 0.95).

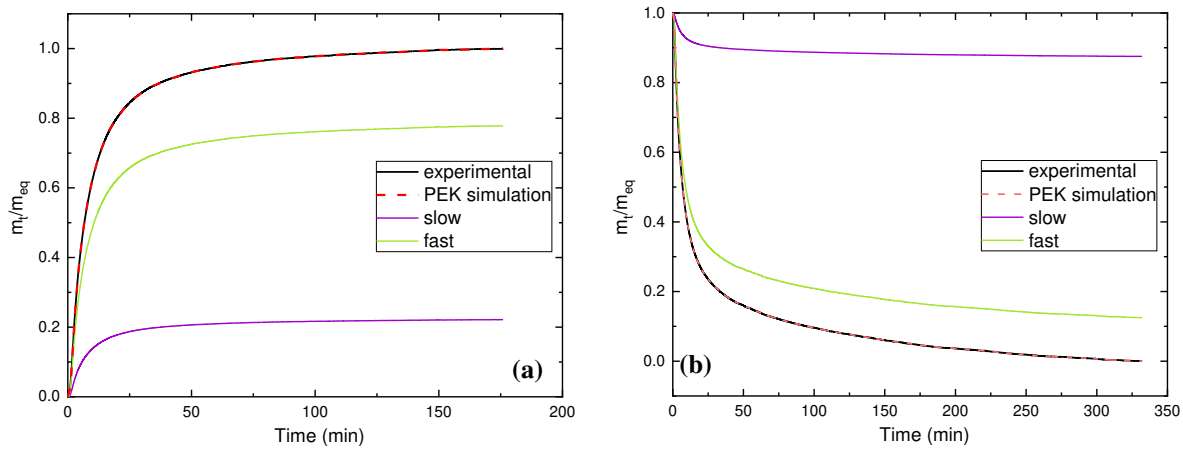


**Fig. 8** PEK simulations of experimental data of $m_t/m_{eq}$ with contribution of slow and fast process for **(a)** sorption (from $a_w$= 0.2 to 0.3) and **(b)** desorption (from $a_w$= 0.3 to 0.2) for C at 25 °C

The obtained characteristic times are the inverse of kinetic rate constants and are certainly related to diffusion coefficients (Kohler et al. 2006), so a high characteristic time means a low process rate. Thus, kinetic rates increase, then stay constant and finally decrease. This trend has already been reported in the literature for hydrophilic materials (Gouanvé et al. 2006; Alix et al. 2009; Bessadok et al. 2009; Belbekhouche et al. 2011) and it is in agreement with the three consecutive steps of a BET type II sorption mechanism (Langmuir, Henry and aggregation). The increase of the kinetic rate for a low water content can be explained by the double sorption mode (Langmuir + Henry). Water molecules predominately were sorbed in Langmuir's sites (specific sites of interactions) in which they were partially or totally immobilized. Then, Henry's type adsorption becomes dominant and the sorption rate increases until a constant value. The decrease of sorption rate has been explained in 1947 by Rouse (Barrie and Platt; Rouse 1940) as the consequence of aggregation of water molecules. This can be assigned to the increase of cluster size of the diffuse species which become less mobile. This trend has already been observed by Gouanvé et al. (Gouanvé et al. 2007).

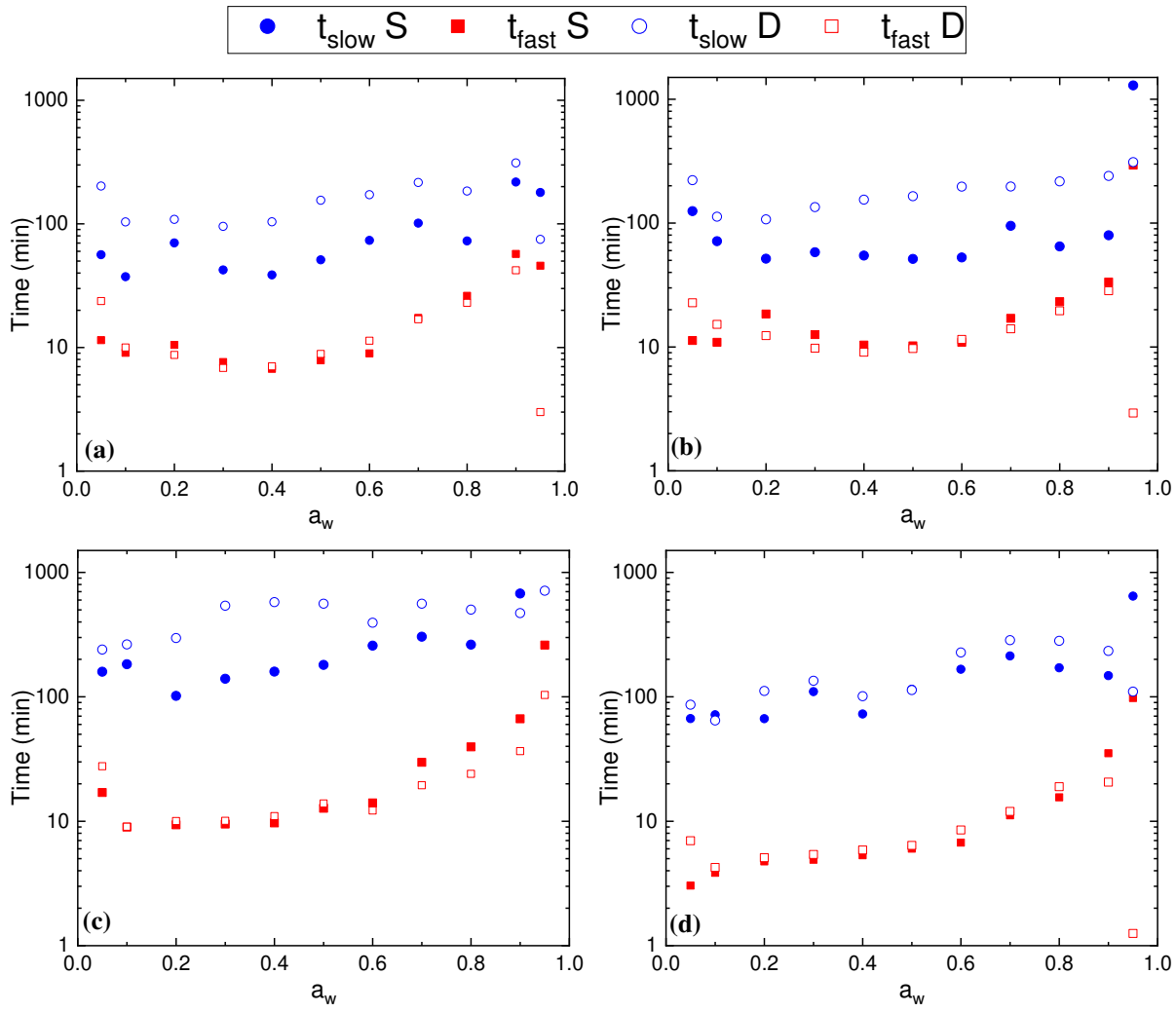


**Fig. 9** Variation of characteristics times for the fast and slow adsorption and desorption processes versus RH for **(a)** C, **(b)** F, **(c)** V and **(d)** CA fibers

For CA, $t_{Fast}$.and $t_{Slow}$ for sorption and desorption are relatively constant until $a_w = 0.6$ and then increase at high water activity (0.6 to 0.95). The non-occurrence of the decrease of characteristic times at low water activity was due to the low amount of sorption sites of CA fibers because hydroxyl groups are substituted by acetyl groups (Popescu et al. 2014).

Characteristic times were compared for the sorption and desorption to determine the effect on the kinetic rate. For C, F and V, $t_{Fast}$ for sorption ($t_{Fast}$ S) and desorption ($t_{Fast}$ D) are almost constant meaning that the fast process is similar. For the slow process, in the whole range of water activity, $t_{Slow}$ D are always higher than $t_{Slow}$ S meaning that the kinetic rate was higher for sorption than desorption. This trend has already been observed by Kohler et al. (Kohler et al. 2003) and Hill et al.(Xie et al. 2011b).

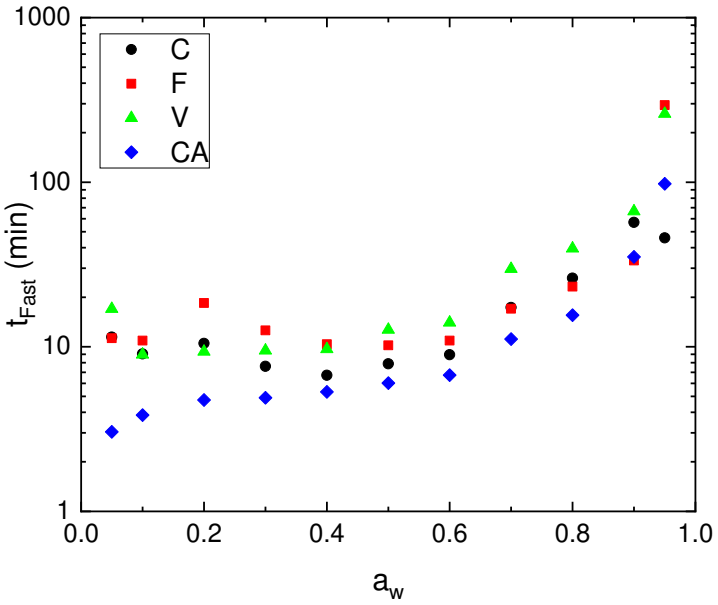


**Fig. 10** Variation of characteristics times for fast sorption processes versus $a_w$ for C, F, V and CA fibers

The differences among cellulosic fibers in the fast process behavior are more clearly illustrated when the curves are overlaid in **Fig. 10**. The characteristic times are close to each other for C, F and V, in the whole range of water activity meaning that the fast sorption process is similar. Lower values of $t_{Fast}$ were obtained for CA meaning that the kinetic sorption rate is higher. This result can be explained by a lower affinity of water molecules due to the decrease of the hydroxyl groups within the fibers.

## Conclusions

This study has shown that there are considerable differences in the sorption/desorption behavior between cellulosic derivatives. Hydrophilic behavior of cellulosic materials depends on their composition and their structural properties. More specifically, it depends on the amount of sorption sites (hydroxyl groups) and the amorphous fraction. To understand the sorption mechanisms from the thermodynamic and kinetic point of view, Park and PEK model were used respectively.

V fibers isotherms shown the highest water sorption capacity allowed by the greatest hydroxyl groups accessibility and the large fraction of amorphous phase, followed by flax and cotton which have a more crystalline structure. Cellulose acetate, due to the hydroxyl substitution into acetyl groups, exhibited the lowest water content despite its low crystallinity. The Park model provides extremely good fits to the experimental data over the entire range of water activity for the all cellulosic fibers. The Park's model parameters were compared for the sorption and desorption isotherms for each fiber. Regardless the fiber nature, differences were obtained only for the Henry sorption.

The sorption and desorption kinetic curves were analyzed by using the PEK model which has provided excellent fits for the all cellulosic fibers. Regarding characteristic times, similar trend was noticed for sorption and desorption which agree with the BET isotherm. Similar characteristic times $t_{Fast}$ were found in sorption and desorption but different behaviors were observed in sorption and desorption for the slow process. This difference is linked to the presence of sorption sites and their accessibility.

## Acknowledgment

The authors gratefully acknowledge Ruben Vera and the Centre de Diffractométrie Henri Longchambon of Univeristy of Lyon 1 for the reflection XRD experiments.

## Funding

This work was supported by FUI (*Fonds Unique Interministériel*) of the French government and the European Regional Development Fund (FEDER) of Region aura through the PLUG&WET project led by "Les Tissages de Charlieu"

## Conflicts of interest/Competing interests

The authors declare no conflict of interest.

## Compliance with Ethical Standards

No animal studies or human participants involvement in the study

## Availability of data and material (data transparency)

All data and materials as well as software application or custom code support published claims and comply with field standards.

## Authors' contributions

Conceptualization: [René Fulchiron], [Fabrice Gouanvé]; Methodology: [Mathilde Simon], [René Fulchiron], [Fabrice Gouanvé]; Formal analysis and investigation: [Mathilde Simon]; Writing - original draft preparation: [Mathilde Simon], [René Fulchiron], [Fabrice Gouanvé]; Funding acquisition: [René Fulchiron], [Fabrice Gouanvé]; Resources: [René Fulchiron] [Fabrice Gouanvé]; Supervision: [René Fulchiron] [Fabrice Gouanvé]

## References

Abidi N, Cabrales L, Haigler CH (2014) Changes in the cell wall and cellulose content of developing cotton fibers investigated by FTIR spectroscopy. Carbohydr Polym 100:9–16. https://doi.org/10.1016/j.carbpol.2013.01.074

Al-Muhtaseb AH, McMinn WAMM, Magee TRAA (2004) Water sorption isotherms of starch powders: Part 1: Mathematical description of experimental data. J Food Eng 61:297–307. https://doi.org/10.1016/S0260-8774(03)00133-X

Alix S, Philippe E, Bessadok A, et al (2009) Effect of chemical treatments on water sorption and mechanical properties of flax fibres. Bioresour Technol 100:4742–4749. https://doi.org/10.1016/j.biortech.2009.04.067

Arbelaiz A, Cantero G, Fernández B, et al (2005) Flax fiber surface modifications: Effects on fiber physico mechanical and flax/polypropylene interface properties. Polym Compos 26:324–332. https://doi.org/10.1002/pc.20097

435 Awais H, Nawab Y, Amjad A, et al (2021) Environmental benign natural fibre reinforced thermoplastic
436 composites: A review. Compos Part C Open Access 4:100082. https://doi.org/10.1016/j.jcomc.2020.100082

437 Barrie JA, Platt B The Diffusion and Clustering of Water Vapour in Polymers. 303–313

438 Basu S, Shivhare US, Mujumdar AS (2006) Models for sorption isotherms for foods: A review. Dry Technol
439 24:917–930. https://doi.org/10.1080/07373930600775979

440 Beever DK, Valentine L (2007) Studies on the sorption of moisture by polymers. II. The cellulose-cellulose acetate
441 system. J Appl Chem 8:103–107. https://doi.org/10.1002/jctb.5010080204

442 Belbekhouche S, Bras J, Siqueira G, et al (2011) Water sorption behavior and gas barrier properties of cellulose
443 whiskers and microfibrils films. Carbohydr Polym 83:1740–1748.
444 https://doi.org/10.1016/j.carbpol.2010.10.036

445 Bessadok A, Langevin D, Gouanvé F, et al (2009) Study of water sorption on modified Agave fibres. Carbohydr
446 Polym 76:74–85. https://doi.org/10.1016/j.carbpol.2008.09.033

447 Bledzki A. K, Gassan J (1999) Composites reinforced with cellulose. Prog Polym Sci 24:221–274

448 Carrillo-Varela I, Pereira M, Mendonça RT (2018) Determination of polymorphic changes in cellulose from
449 Eucalyptus spp. fibres after alkalization. Cellulose 25:6831–6845. https://doi.org/10.1007/s10570-018-
450 2060-4

451 Célino A, Fréour S, Jacquemin F, Casari P (2014) The hygroscopic behavior of plant fibers: A review. Front Chem
452 1:1–12. https://doi.org/10.3389/fchem.2013.00043

453 Célino A, Fréour S, Jacquemin F, Casari P (2013) Characterization and modeling of the moisture diffusion
454 behavior of natural fibers. J Appl Polym Sci 130:297–306. https://doi.org/10.1002/app.39148

455 Chirife J, Fontan CF, Benmergui EA (1980) The prediction of water activity in aqueous solutions in connection
456 with intermediate moisture foods IV. aW Prediction in aqueous non electrolyte solutions. Int J Food Sci
457 Technol 15:59–70. https://doi.org/10.1111/j.1365-2621.1980.tb00919.x

458 Cunha AG, Zhou Q, Larsson PT, Berglund LA (2014) Topochemical acetylation of cellulose nanopaper structures
459 for biocomposites: Mechanisms for reduced water vapour sorption. Cellulose 21:2773–2787.
460 https://doi.org/10.1007/s10570-014-0334-z

461 Das AM, Ali AA, Hazarika MP (2014) Synthesis and characterization of cellulose acetate from rice husk: Eco-
462 friendly condition. Carbohydr Polym 112:342–349. https://doi.org/10.1016/j.carbpol.2014.06.006

463 Davis EM, Elabd YA (2013) Water clustering in glassy polymers. J Phys Chem B 117:10629–10640.
464 https://doi.org/10.1021/jp405388d

465 Deus C, Friebolin H, Siefert E (1991) Partiell acetylierte cellulose — synthese und bestimmung der
466 substituentenverteilung mit hilfe der 1H NMR-spektroskopie. Die Makromol Chemie 192:75–83.
467 https://doi.org/10.1002/macp.1991.021920107

Duchemin B, Thuault A, Vicente A, et al (2012) Ultrastructure of cellulose crystallites in flax textile fibres. Cellulose 19:1837–1854. https://doi.org/10.1007/s10570-012-9786-1

Dunne R, Desai D, Sadiku R, Jayaramudu J (2016) A review of natural fibres, their sustainability and automotive applications. J Reinf Plast Compos 35:1041–1050. https://doi.org/10.1177/0731684416633898

Farahnaky A, Ansari S, Majzoobi M (2009) Effect of glycerol on the moisture sorption isotherms of figs. J Food Eng 93:468–473. https://doi.org/10.1016/j.jfoodeng.2009.02.014

Freire CSR, Silvestre AJD, Neto CP, et al (2006) Controlled heterogeneous modification of cellulose fibers with fatty acids: Effect of reaction conditions on the extent of esterification and fiber properties. J Appl Polym Sci 100:1093–1102. https://doi.org/10.1002/app.23454

French AD (2017) Glucose, not cellobiose, is the repeating unit of cellulose and why that is important. Cellulose 24:4605–4609. https://doi.org/10.1007/s10570-017-1450-3

French AD (2014) Idealized powder diffraction patterns for cellulose polymorphs. Cellulose 21:885–896. https://doi.org/10.1007/s10570-013-0030-4

Gocho H, Shimizu H, Tanioka A, et al (2000) Effect of acetyl content on the sorption isotherm of water by cellulose acetate: Comparison with the thermal analysis results. Carbohydr Polym 41:83–86. https://doi.org/10.1016/S0144-8617(99)00112-5

Gouanvé F, Marais S, Bessadok A, et al (2006) Study of water sorption in modified flax fibers. J Appl Polym Sci 101:4281–4289. https://doi.org/10.1002/app.23661

Gouanvé F, Marais S, Bessadok A, et al (2007) Kinetics of water sorption in flax and PET fibers. Eur Polym J 43:586–598. https://doi.org/10.1016/j.eurpolymj.2006.10.023

Guggenheim EA (1966) Applications of statistical mechanics

Guo X, Wu Y, Xie X (2017) Water vapor sorption properties of cellulose nanocrystals and nanofibers using dynamic vapor sorption apparatus. Sci Rep 7:1–12. https://doi.org/10.1038/s41598-017-14664-7

Hill CAS (2006) Wood Modification: Chemical, Thermal and Other Processes

Hill CAS, Norton A, Newman G (2009) The water vapor sorption behavior of natural fibers. J Appl Polym Sci 112:1524–1537. https://doi.org/10.1002/app29725

Hill CASS, Norton A, Newman G (2010a) Analysis of the water vapour sorption behaviour of Sitka spruce [Picea sitchensis (Bongard) Carr.] based on the parallel exponential kinetics model. Holzforschung 64:469–473. https://doi.org/10.1515/HF.2010.059

Hill CASS, Norton A, Newman G (2010b) The water vapor sorption behavior of Flax fibers- analysis using the parallel exponential kinetics model and determination of the activation energies of sorption. J Appl Polym Sci 116:2658–2667. https://doi.org/10.1002/app

Hill CASS, Norton AJ, Newman G (2010c) The water vapour sorption properties of Sitka spruce determined using

501 a dynamic vapour sorption apparatus. Wood Sci Technol 44:497–514. https://doi.org/10.1007/s00226-010-
502 0305-y

503 Hill CASS, Xie Y (2011) The dynamic water vapour sorption properties of natural fibres and viscoelastic
504 behaviour of the cell wall: Is there a link between sorption kinetics and hysteresis? J Mater Sci 46:3738–
505 3748. https://doi.org/10.1007/s10853-011-5286-1

506 Himmel S, Mai C (2016) Water vapour sorption of wood modified by acetylation and formalisation - Analysed by
507 a sorption kinetics model and thermodynamic considerations. Holzforschung 70:203–213.
508 https://doi.org/10.1515/hf-2015-0015

509 Hindeleh AM, Johnson DJ (1974) Crystallinity and crystallite size measurement in cellulose fibres: 2. Viscose
510 rayon. Polymer (Guildf) 15:697–705. https://doi.org/10.1016/0032-3861(74)90020-2

511 Hu W, Chen S, Xu Q, Wang H (2011) Solvent-free acetylation of bacterial cellulose under moderate conditions.
512 Carbohydr Polym 83:1575–1581. https://doi.org/10.1016/j.carbpol.2010.10.016

513 Ibbett RN, Domvoglou D, Phillips DAS (2008) The hydrolysis and recrystallisation of lyocell and comparative
514 cellulosic fibres in solutions of mineral acid. Cellulose 15:241–254. https://doi.org/10.1007/s10570-007-
515 9157-5

516 Iglesias HA, Chirife J (1976) A Model for Describing the Water Sorption Behavior of Foods. J Food Sci 41:984–
517 992. https://doi.org/10.1111/j.1365-2621.1976.tb14373.x

518 Jonquières A, Fane A (1998) Modified BET models for modeling water vapor sorption in hydrophilic glassy
519 polymers and systems deviating strongly from ideality. J Appl Polym Sci 67:1415–1430.
520 https://doi.org/10.1002/(sici)1097-4628(19980222)67:8<1415::aid-app7>3.0.co;2-h

521 K. Kaushik V, Kumar A, Kalia S (2013) Effect of Mercerization and Benzoyl Peroxide Treatment on Morphology,
522 Thermal Stability and Crystallinity of Sisal Fibers. Int J Text Sci 1:101–105.
523 https://doi.org/10.5923/j.textile.20120106.07

524 Kabir MM, Wang H, Lau KT, Cardona F (2012) Chemical treatments on plant-based natural fibre reinforced
525 polymer composites: An overview. Compos Part B Eng 43:2883–2892.
526 https://doi.org/10.1016/j.compositesb.2012.04.053

527 Kafle K, Greeson K, Lee C, Kim SH (2014) Cellulose polymorphs and physical properties of cotton fabrics
528 processed with commercial textile mills for mercerization and liquid ammonia treatments. Text Res J
529 84:1692–1699. https://doi.org/10.1177/0040517514527379

530 Kale RD, Gorade VG, Parmaj O (2020) Novel Sericin/Viscose Rayon-Based Biocomposite: Preparation and
531 Characterization. J Nat Fibers 17:532–541. https://doi.org/10.1080/15440478.2018.1503131

532 Karacan I, Soy T (2013) Investigation of structural transformations taking place during oxidative stabilization of
533 viscose rayon precursor fibers prior to carbonization and activation. J Mol Struct 1041:29–38.
534 https://doi.org/10.1016/j.molstruc.2013.02.040

Khali DP, Rawat SPS (2000) Clustering of water molecules during adsorption of water in brown rot decayed and undecayed wood blocks of Pinus sylvestris. Holz als Roh - und Werkst 58:340–341. https://doi.org/10.1007/s001070050441

Klemm D, Heublein B, Fink HP, Bohn A (2005) Cellulose: Fascinating biopolymer and sustainable raw material. Angew Chemie - Int Ed 44:3358–3393. https://doi.org/10.1002/anie.200460587

Kohler R, Alex R, Brielmann R, Ausperger B (2006) A new kinetic model for water sorption isotherms of cellulosic materials. Macromol Symp 244:89–96. https://doi.org/10.1002/masy.200651208

Kohler R, Dück R, Ausperger B, Alex R (2003) A numeric model for the kinetics of water vapor sorption on cellulosic reinforcement fibers. Compos Interfaces 10:255–276. https://doi.org/10.1163/156855403765826900

Kostag M, Gericke M, Heinze T, El Seoud OA (2019) Twenty-five years of cellulose chemistry: innovations in the dissolution of the biopolymer and its transformation into esters and ethers. Springer Netherlands

Krabbenhoft K, Damkilde L (2004) A model for non-Fickian moisture transfer in wood. Mater Struct Constr 37:615–622. https://doi.org/10.1617/14036

Labuza TP (1980) The effect of water activity on reaction kinetics of food deterioration. Food Technol 34:36-41,59

Leung H (1983) Water activity and other colligative properties of foods. In: ASAE Annual Meeting. Chiacago, p 6508

Lilholt H, Lawther JM (2000) Natural Organic Fibers. Compr Compos Mater 303–325

Lomauro CJ, Bakshi AS, Labuza TP (1985) Evaluation of food moisture sorption isotherm equations 1. Fruit, vegetable and meat-products. Leb Wissenchaft Technol 18:111–117

Lundberg JL (1972) Molecular Clustering And Segregation In Sorption Systems. Pure Appl Chem 31:261–282. https://doi.org/10.1351/pac197231010261

Manian AP, Pham T, Bechtold T (2018) Regenerated cellulosic fibers. Handb Prop Text Tech Fibres 329–343. https://doi.org/10.1016/B978-0-08-101272-7.00010-9

Masclaux C, Gouanvé F, Espuche E (2010) Experimental and modelling studies of transport in starch nanocomposite films as affected by relative humidity. J Memb Sci 363:221–231. https://doi.org/10.1016/j.memsci.2010.07.032

Mihranyan A, Llagostera AP, Karmhag R, et al (2004) Moisture sorption by cellulose powders of varying crystallinity. Int J Pharm 269:433–442. https://doi.org/10.1016/j.ijpharm.2003.09.030

Mikhalovska LI, Gun'Ko VM, Rugal AA, et al (2012) Cottonised flax fibres vs. cotton fibres: Structural, textural and adsorption characteristics. RSC Adv 2:2032–2042. https://doi.org/10.1039/c2ra00725h

Mohanty AK, Misra M, Hinrichsen G (2000) Biofibres, biodegradable polymers and biocomposites: An overview.

568 Macromol Mater Eng 276–277:1–24. https://doi.org/10.1002/(SICI)1439-2054(20000301)276:1<1::AID-
569 MAME1>3.0.CO;2-W

570 Mozdyniewicz DJ, Nieminen K, Kraft G, Sixta H (2016) Degradation of viscose fibers during acidic treatment.
571 Cellulose 23:213–229. https://doi.org/10.1007/s10570-015-0796-7

572 Okubayashi S, Griesser UJ, Bechtold T (2005a) Moisture sorption/desorption behavior of various manmade
573 cellulosic fibers. J Appl Polym Sci 97:1621–1625. https://doi.org/10.1002/app.21871

574 Okubayashi S, Griesser UJ, Bechtold T (2004) A kinetic study of moisture sorption and desorption on lyocell
575 fibers. Carbohydr Polym 58:293–299. https://doi.org/10.1016/j.carbpol.2004.07.004

576 Okubayashi S, Griesser UJ, Bechtold T (2005b) Water accessibilities of man-made cellulosic fibers - Effects of
577 fiber characteristics. Cellulose 12:403–410. https://doi.org/10.1007/s10570-005-2179-y

578 Olesen PO, Placket DV (1999) Perspectives on the performance of natural plant fibres. Nat Fibres Perform Forum
579 7

580 Ormondroyd GA, Curling SF, Mansour E, Hill CASS (2017) The water vapour sorption characteristics and kinetics
581 of different wool types. J Text Inst 108:1198–1210. https://doi.org/10.1080/00405000.2016.1224442

582 Park GS (1986) Transport Principles solution, diffusion and permeation in polymer membranes. Synth Membr Sci
583 Eng Appl 57–107. https://doi.org/10.1007/978-94-009-4712-2_3

584 Park S, Baker JO, Himmel ME, et al (2010) Cellulose crystallinity index: Measurement techniques and their impact
585 on interpreting cellulase performance. Biotechnol Biofuels 3:1–10. https://doi.org/10.1186/1754-6834-3-10

586 Peleg M (1993) Assessment of a semo-empirical four parameter general model for sigmoid moisture sorption
587 isotherms. J Food Process Eng 16:21–37. https://doi.org/10.1111/j.1745-4530.1993.tb00160.x

588 Popescu CM, Hill CAS, Curling S, et al (2014) The water vapour sorption behaviour of acetylated birch wood:
589 How acetylation affects the sorption isotherm and accessible hydroxyl content. J Mater Sci 49:2362–2371.
590 https://doi.org/10.1007/s10853-013-7937-x

591 Ramamoorthy SK, Skrifvars M, Persson A (2015) A review of natural fibers used in biocomposites: Plant, animal
592 and regenerated cellulose fibers. Polym Rev 55:107–162. https://doi.org/10.1080/15583724.2014.971124

593 Reddy KM, Manorama S V., Reddy AR (2003) Bandgap studies on anatase titanium dioxide nanoparticles. Mater
594 Chem Phys 78:239–245. https://doi.org/10.1016/S0254-0584(02)00343-7

595 Rodrigues Filho G, Monteiro DS, Meireles C da S, et al (2008) Synthesis and characterization of cellulose acetate
596 produced from recycled newspaper. Carbohydr Polym 73:74–82.
597 https://doi.org/10.1016/j.carbpol.2007.11.010

598 Rouse PE (1940) Diffusion of vapors in Films. J Am Chem Soc 69:1068–1073.
599 https://doi.org/10.1021/ja01197a029

600 Sabard M, Gouanvé F, Espuche E, et al (2012) Influence of film processing conditions on the morphology of

polyamide 6: Consequences on water and ethanol sorption properties. J Memb Sci 415–416:670–680. https://doi.org/10.1016/j.memsci.2012.05.048

Sanjay MR, Siengchin S, Parameswaranpillai J, et al (2019) A comprehensive review of techniques for natural fibers as reinforcement in composites: Preparation, processing and characterization. Carbohydr Polym 207:108–121. https://doi.org/10.1016/j.carbpol.2018.11.083

Smith SE, Smith SE (1947) The Sorption of Water Vapor by High Polymers. J Am Chem Soc 69:646–651. https://doi.org/10.1021/ja01195a053

Terinte N, Ibbett R, Schuster KC (2011) Overview on Native Cellulose and Microcrystalline Cellulose I Structure Studied By X-Ray Diffraction (WAXD): Comparison Between Measurement Techniques. Lenzinger Berichte 89:118–131. https://doi.org/10.1163/156856198X00740

Thygesen A, Oddershede J, Lilholt H, et al (2005) On the determination of crystallinity and cellulose content in plant fibres. Cellulose 12:563–576. https://doi.org/10.1007/s10570-005-9001-8

Van Der Wel GK, Adan OCG (1999) Moisture in organic coatings - a review. Prog Org Coatings 37:1–14. https://doi.org/10.1016/S0300-9440(99)00058-2

Wolf C, Guillard V, Angellier-Coussy H, et al (2016) Water vapor sorption and diffusion in wheat straw particles and their impact on the mass transfer properties of biocomposites. J Appl Polym Sci 133:1–10. https://doi.org/10.1002/app.43329

Wu S, Qin X, Li M (2014) The structure and properties of cellulose acetate materials: A comparative study on electrospun membranes and casted films. J Ind Text 44:85–98. https://doi.org/10.1177/1528083713477443

Xie Y, Hill CAS, Jalaludin Z, et al (2011a) The dynamic water vapour sorption behaviour of natural fibres and kinetic analysis using the parallel exponential kinetics model. J Mater Sci 46:479–489. https://doi.org/10.1007/s10853-010-4935-0

Xie Y, Hill CAS, Xiao Z, et al (2010) Water vapor sorption kinetics of wood modified with glutaraldehyde. J Appl Polym Sci 117:1674–1682. https://doi.org/10.1002/app

Xie Y, Hill CAS, Xiao Z, et al (2011b) Dynamic water vapour sorption properties of wood treated with glutaraldehyde. Wood Sci Technol 45:49–61. https://doi.org/10.1007/s00226-010-0311-0

Xie Y, Hill CASS, Jalaludin Z, Sun D (2011c) The water vapour sorption behaviour of three celluloses: Analysis using parallel exponential kinetics and interpretation using the Kelvin-Voigt viscoelastic model. Cellulose 18:517–530. https://doi.org/10.1007/s10570-011-9512-4

Yueping W, Ge W, Haitao C, et al (2010) Structures of Bamboo Fiber for Textiles. Text Res J 80:334–343. https://doi.org/10.1177/0040517509337633

Zeppa C, Gouanvé F, Espuche E (2009) Effect of a plasticizer on the structure of biodegradable Starch/Clay nanocomposites: Thermal, water-sorption, and Oxygen-Barrier properties. J Appl Polym Sci 112:2044–2056. https://doi.org/10.1002/app

635 Zimm BH, Lundberg JL (1956) Sorption of vapors by high polymers. J Phys Chem 60:425–428.
636 https://doi.org/10.1021/j150538a010

637

## Supplementary Files

This is a list of supplementary files associated with this preprint. Click to download.

- Article1Supportinginformation.docx